Earth, Moon, and Planets (2004) 95: 501–512
DOI 10.1007/s11038-005-2244-4

BOLIDE ENERGY ESTIMATES FROM INFRASONIC MEASUREMENTS

WAYNE N. EDWARDS
Department of Earth Sciences, University of Western Ontario, London, Ontario N6A 5B7, Canada

PETER G. BROWN
Canada Research Chair in Meteor Science, Department of Physics and Astronomy, University of Western Ontario, London, Ontario N6A 3K7, Canada

DOUGLAS O. REVELLE
Atmospheric, Climate and Environmental Dynamics, Meteorological Modeling Team, P.O. Box 1663, MS D401, Los Alamos National Laboratory, Los Alamos, New Mexico 87545 USA

(Accepted 14 February 2005)

Abstract. The acoustic amplitude-yield relationships, including formal errors, for a population of energetic (>0.05 kt) and well-observed bolide events have been investigated. Using various infrasonic signal measurements as a function of range, these data have been calibrated against optical yield estimates from satellite measurements. Correction for the presence of stratospheric winds has also been applied to the observations and is found to be small, suggesting that either scatter is dominated by other variations amongst the fireball population such as differing burst altitudes and greater or lesser amounts of fragmentation or the magnitude of the variability in the stratospheric winds, which can be comparable to or even exceed the strength of the winds themselves. Comparison to similar point source, ground-level nuclear and high explosive airwave data shows that bolide infrasound is consistently lower in amplitude. This downward shift relative to nuclear and HE data is interpreted as due in part to increased weak non-linearity during signal propagation from higher altitudes. This is a likely explanation, since mean estimates of the altitude of maximum energy deposition along the bolide trajectory was found to be between 20 and 30 km altitude for this fireball population.

1. Introduction

Infrasonic sound (0.01 to ~20 Hz) produced by large meteoroids (0.1–1 m diameters) entering the Earth's atmosphere at hypersonic velocities has been a subject of interest for many researchers since the occurrence of the 1908 Tunguska blast in Siberia (Ben-Menahem, 1975). Produced either by the shock front of the entering meteoroid or by subsequent fragmentation of the object at altitude, several authors have reported the recording of meteor infrasound by microbarometer arrays in the past (e.g. ReVelle, 1976; Brown et al., 2002a; Pichon et al., 2002). However, until recently the number of microbarometer arrays has been very small. This has changed over the past several years with the construction of the international monitoring network

as part of the Comprehensive Test Ban Treaty Organization (CTBTO) whose purpose is to monitor for nuclear explosions worldwide. Additionally, with the release of U.S. Department of Defense (DoD) and Department of Energy (DoE) satellite optical data for several bolides, it has become possible to calibrate infrasound observations using an independent measurement for the initial energy of the bolide (Brownet al., 2002b).

Historically, observations of infrasound from bolides have been triggered by the ground observations of eyewitnesses (be they casual, photographic or video) and dedicated fireball camera networks. Although these systems remain an important tool for fireball investigation, they suffer from various limitations when attempting to determine the energy of a bolide. Casual eyewitness testimony and photographs often only delimit a bolide's trajectory, without providing velocity information. Eyewitness video offers a potentially much better record, especially in determining velocity, but suffers from issues related to the need for calibration, orientation and light sensitivity (c.f. Borovička et al., 2004). Dedicated fireball camera networks avoid this continual calibration problem but suffer from the fact that they are stationary systems and must wait for a bolide of sufficient energy to occur nearby. Camera networks also are limited in the total atmospheric area that is monitored making detection of highly energetic events rare. For example, the Canadian Meteorite Observation and Recovery project (MORP) which operated from 1971 to 1985 had the equivalent clear-sky area-time coverage as would be obtained by monitoring the entire globe for 29 h (Halliday et al., 1996). The satellite-based optical sensors of the DoD and DoE combine the best of both worlds, as they cover areas not easily seen by casual observers and have been approximately calibrated for conversion from radiation measured in the silicon bandpass to the total energy of the object (Brown et al., 2002). An outstanding issue in all these calibrations is the unknown applicability of the assumption of a 6000 K blackbody for such large fireball events.

With the public release of DoD and DoE satellite data, it is now possible to study empirically the bolide infrasound phenomena in a way that was never possible before, by cross-calibrating airwave measurements against satellite optical energy estimates, which will provide a means to ground-truth previous bolide infrasound theory.

2. Bolide Data Selection Criteria and Scaling Relations

The database of bolide infrasound has been collected over the past decade using fireball information gleaned from various optical camera networks, published literature and DoD and DoE press releases of satellite observed bolides; a total of ~50 separate bolide events with observed infrasound has

been compiled. For many events, only a single station has detected an infrasonic signal, though a significant fraction (~20%) have been observed by two or more arrays. In addition, for some events, supplemental information is available from independent sources in the form of velocities, optical energy measurements and trajectories/location information. For a few events, meteorites have been recovered on the ground providing the ultimate ground-truth (c.f. Spurný et al., 2003 for an example related to the Neushwanstein meteorite fall) and yet another means to calibrate pre-atmospheric size through radionuclide measurements.

To study the relationship that exists between bolide energy and observed airwave signals, a subset of the bolide infrasound dataset was selected with the goal of removing any possible biases and/or dissimilarities that may exist within the database due to observational range. In particular, only signals observed from a range of >250 km have been included in the subset to isolate only stratospheric arrivals, that is only those waves that have refracted back to the ground at least once from the stratosphere. Similarly, only airwave signals having a minimum average signal velocity >0.28 km/s were included, to remove thermospheric returns (waves refracting to the ground from the thermosphere) (Ceplecha et al., 1998) or stratospheric arrivals with exceptionally strong counter-winds. In general, thermospheric returns were not commonly observed as our average observed range of 3000 km results in severe attenuation for thermospheric returns., Thus all signals in the subset comprise only stratospherically ducted waves.

In addition to these observational range/travel time restrictions, the second criteria for selection was that only those events that have been simultaneously observed by DoD and DoE satellite instruments and infrasound were to be included. This criterion was chosen so that for each event, a quasi-independent method could be used to determine the bolide initial energy or yield and thus calibrate the infrasound energy relationship. This is possible for satellite observed bolides due to the relation determined previously by Brown et al. (2002b) between optical and total energy for bolides,

$$\tau_1 = 0.1212 E_0^{0.115} \tag{1}$$

where τ_1 is the integral luminous efficiency and E_0 is the optical energy (in kilotons of TNT equivalent) measured by the satellite sensors assuming that the bolide emission is that of a blackbody with a temperature of 6000 K (Tagliaferri et al., 1994).

After determination of each bolide's initial energy with the associated satellite optical sensor data and Equation (1), a scaling method for comparison of events with different energy observed at differing ranges for airwave data is required. The energy scaling used is adopted from the empirical

results obtained during investigations of free-air nuclear blasts in the 1950s and 1960s. A detailed version of this scaling law is given by ReVelle and Whitaker (1997) relating range and energy directly to the overpressure, which in the linear regime has the form

$$\Delta p = C\left(\frac{p_0}{p}\right)^{-2/3} R^{-1} W^{1/3} \tag{2}$$

where C is a constant, p_0/p is the ratio of pressures at the source and observation altitudes, and R and W are the observational range and source energy (yield), respectively. Treating all quantities except range and yield as constants in Equation (2), and substituting the satellite energy estimates and range, we define a scaled range for each bolide infrasonic observation as

$$R_S = \frac{R}{W^{1/3}} \tag{3}$$

where R is in kilometres and W in tons of TNT equivalent energy. This scaling of the range requires the assumption that at distances greater then the energy deposition length of a moving point source, the source may be approximated by a point source release of energy from a specific altitude (an assumption used to derive Equation (2)).

The physical reasoning behind this scaling of range in Equation (3) comes primarily from the geometry for a point source explosion. If a point source is located at an altitude with pressure, p_0, then the energy released will be distributed initially over a sphere of radius R_B, where

$$R_B = \left(\frac{W}{4/3\pi p_0}\right)^{1/3} \tag{4}$$

This is described as the blast radius of the source, physically interpreted as the zone in which all wave energy propagates in a highly non-linear (shocked) state. Since quantities such as the initial overpressure and the fundamental wave period are proportional to R_B, the scaling factor of 1/3 will tend to appear in the observations of point source type explosions. For many bolides, the majority of the energy deposition occurs over a short length of their total trajectory, often near the end of their luminous flight, so comparison with point-source explosions is valid. This also assumes that the size of the explosion is small when compared to the scale height of the atmosphere (~7 km). For very large explosions this relationship breaks down as the spherical symmetry of the source is lost and internal gravity waves begin to

dominate the atmosphere's response. For most bolides however gravity waves are not the dominant type of observed wave.

3. Measurements, Wind Correction and Results

For each infrasonic observation of a bolide (Table I), several quantities of the waveform were measured after stacking and averaging of the waveform by phase aligning signals measured across the array. Measured quantities included (1) the maximum amplitude of the signal envelope computed from the Hilbert transform of the signal (Dziewonski and Hales, 1972), (2) the maximum peak to peak amplitude of the signal within the maximum signal envelope and (3) period at maximum amplitude computed from the four zero crossings at the location of the peak to peak amplitude in the signal. Computed quantities included (4) an estimate for the infrasonic signal energy or power through summation of the squared amplitudes of the bolide signal from which was subtracted the average of the noise power of equal duration prior to and after the bolide signal and (4) an estimate of the signal to noise ratio as determined from the bolide signal and noise power. It should be noted that the signals reported to have been detected from the Tagish Lake fireball (Brown et al., 2002c) have not been included in the present dataset (Table I). After reexamination of the airwave data and signal properties it was found that Tagish Lake was an extreme outlier in all cases. Indeed, it is probable that these reported airwaves are not associated with the Tagish Lake fireball.

Plotting these measurements as a function of scaled range in log–log space, it was found that nearly all followed a generally linear trend consistent with a power law. Only the period at maximum amplitude showed no dependence upon scaled range. However, these power law trends show significant scatter at all scaled ranges and linear regression of the bolide data display poor fits with r squared (the correlation of the least-squares fit) values ranging between 0.262 and 0.460 (integrated signal energy and signal to noise ratio, respectively) where an r squared value of unity represents a perfect fit. This scatter is due in part to the effects of strong atmospheric winds present in the stratosphere and on modification of the signals during the propagation of the infrasonic signals from their respective source bolides.

To correct for the presence of strong stratospheric winds, the correction factor used by Whitaker (1992) while studying infrasonic propagation from the Miser's Gold high explosive test, is adopted. This correction has the form

$$A_W = 10^{kw} A \tag{5}$$

TABLE I

Bolide events for which optical satellite sensor data (E_o) has been published and stations where associated infrasound has been observed

Bolide	Event date	Event time (UT)	Observing station	Arrival time (UT)	Average HWM winds (m/s)	Satellite optical energy (J)	Reference
Park Forest	27/03/2003	05:50:25	I10CA	06:38:00	25.9	1.42E+11	Brown et al. (2004)
			Blossom Point	06:56:15	−17.8		
Eastern US Bolide	23/07/2001	22:19:00	Blossom Point	22:37:52	−7.6	1.27E+12	1
Pacific Bolide #1	23/04/2001	06:12:00	I59US	08:21:23	1.2	4.6E+12	Brown et al. (2002a)
			DLIAR	08:39:25	3.3		
			SGAR	08:09:27	2.3		
			I26DE	16:25:52	1.8		
			NTS	07:54:52	2.0		
			I57US	07:47:56	2.5		
			I10CA	09:54:22	3.0		
			NVIAR	07:52:43	1.4		
Pacific Bolide #2	25/08/2000	01:12:25	I59US	05:53:16	29.3	1.4E+12	Brown et al. (2002a)
			DLIAR	03:24:31	2.0		
			I10CA	05:04:30	−5.7		
			PDIAR	04:08:17	4.1		
Moravka	06/05/2000	11:51:50	I26DE	12:11:27	7.6	2.5E+09	Brown et al. (2003)
El Paso	09/10/1997	18:47:15	DLIAR	19:20:00	7.9	1.9E+11	Hildebrand et al. (1999) ReVelle et al. (1998)

In addition average HWM wind component along the connecting source – receiver great circle path used in data corrections are given for each station. 1- http://aquarid.physics.uwo.ca/~pbrown/usaf.html

where A is the measured quantity, w is the component of the wind vector along the propagation path and k is a constant to be determined from the data. For a value of the component of wind we use an average of the peak wind component between 35 and 60 km altitude sampled every 25 km along the great circle path that connects the source bolide to the infrasound receiver as computed by the Naval Labs Horizontal Wind Model (HWM) (Hedin et al., 1996), as opposed to the SCI component (Webb, 1966, p. 140) used by Whitaker (1992). Note that for this application a positive component is defined as a wind vector pointed in the same direction as the vector going from source to receiver.

Applying this correction for a range of values for k, these data were regressed iteratively for each k until a peak in the r-squared value was found corresponding to the lowest total scatter in these data. Using this procedure r squared values increased significantly from 20% (signal to noise) to 50% (integrated signal energy) with k values of −0.0181 s/m for both maximum signal envelope and peak to peak amplitudes, −0.0369 s/m for integrated signal energy and −0.0106 s/m for signal to noise ratio. Note that the k value for integrated energy (power) are nearly identically twice that of the independently measured amplitude's value for k, consistent with power being proportional to the square of amplitude. This is a reassuring check that this wind correction is not simply a statistical convenience, but that it has its basis in a physical effect.

With wind corrections applied to each infrasonic observation, the power-law curves, along their respective confidence bounds, are obtained (Figures 1–4). The remaining scatter around the calibration curves may in large part

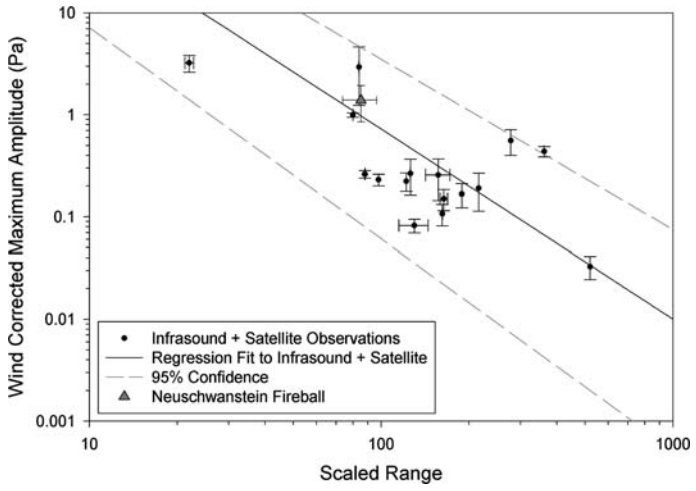

Figure 1. Wind corrected maximum amplitude of the signal envelope for bolide infrasound. $r^2 = 0.584$.

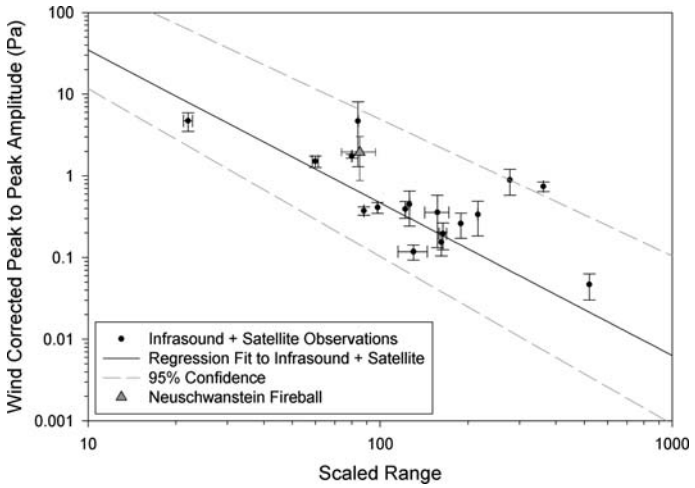

Figure 2. Wind corrected peak to peak amplitude for bolide infrasound. $r^2 = 0.607$.

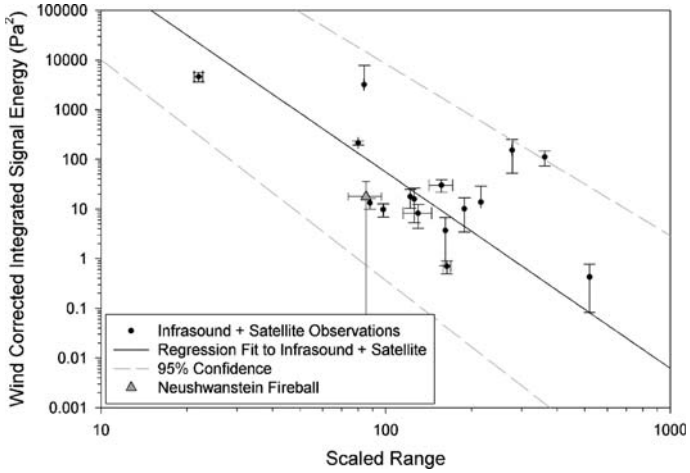

Figure 3. Wind corrected integrated signal energy/power for bolide infrasound. $r^2 = 0.480$.

be due to the uncertainty in the modelled stratospheric winds used. The wind correction term depends greatly on HWM providing accurate wind estimates to the actual wind conditions present at the time of an event, this may or may not be the case for all observations, particularly those that show the presence of strong winds where the correction is greatest (e.g. Park Forest). Finally, from the regression curves and Equation (3), it becomes possible to invert for the bolide source's initial energy directly from the infrasonic observation, these equations have the form:

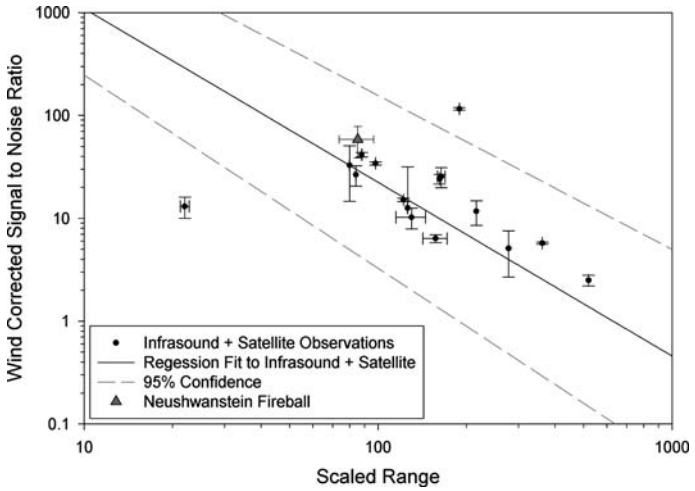

Figure 4. Wind corrected signal to noise ratio for bolide infrasound. $r^2 = 0.548$.

$$W = 10^{-3(a+bw)/c} R^3 A^{3/c} \tag{6}$$

where R is range in kilometres and W is the initial bolide energy in tons of equivalent TNT (1 ton equivalent. TNT $= 4.185 \times 10^9$ J), A is the infrasound signal property, while a, b and c are the regression constants and wind correction constant specific to each measured quantity (Table II).

4. Discussion and Conclusions

As an independent check on the satellite-observed energy calibration, the observed infrasound from the recent Neushwanstein fireball at the Freyung, Germany array (I26DE) was plotted alongside satellite + infrasound data using a bolide energy as calculated from the initial velocity and mass estimates of the meteoroid determined by Spurný et al. (2003). In all four measurement curves (Figures 1–4), the Neushwanstein data falls very near

Table II
Regression constants and wind correction factors found for each bolide infrasound signal property

	Max amplitude of signal envelope (Pa)	Peak to peak amplitude (Pa)	Integrated signal energy/power (Pa^2)	Integrated energy signal to noise ratio
a	3.41 ± 0.48	3.58 ± 0.46	9.64 ± 1.2	4.73 ± 0.46
b	0.0181 s/m	0.0181 s/m	0.0369 s/m	0.0106 s/m
c	1.87 ± 0.20	1.86 ± 0.19	3.95 ± 0.49	1.69 ± 0.19

the satellite + infrasound regression curve, providing confidence that the choice of bolide energy as computed from optical luminous efficiency is robust.

Now that it has become possible to examine bolide infrasound in a statistical sense, a comparison to similar man-made impulsive sources of infrasound in the atmosphere may provide insight into aspects of bolide infrasound that may be unique to this type of natural source. If the regression fit to the bolide peak to peak amplitude is compared alongside similar data from nuclear and high explosive data for standard 1 kt and 2500 lbs (1134 kg) yields, respectively (Reed, 1977), it is found that the bolide curve is significantly steeper and lies beneath both curves in the region where most bolide data are available (Figure 5). Thus it appears that bolide infrasound is more effectively attenuated then man-made explosive infrasound and is commonly observed at lower amplitudes then might otherwise be expected.

One possible explanation of this discrepancy between nuclear-high explosive and bolide infrasound may be the generally higher altitudes from which bolide infrasound is generated. Nuclear and high explosive data have commonly had sources at or near ground level, while in contrast typical bolides have terminal points at a range of altitudes from 15 to 40 km. Higher source altitudes for infrasound requires that as the waves conserve energy in propagating from altitude to the surface through an increasingly dense atmosphere, the signal amplitudes should decrease. Thus when detected at the surface the amplitude is smaller then would be expected for an equivalent

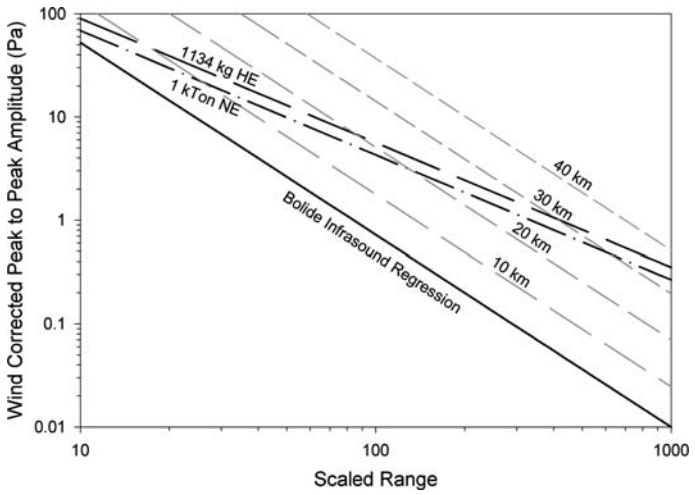

Figure 5. Comparison of bolide peak to peak amplitude to similar empirically derived curves for a 1 kt ground-level nuclear explosion and 1134 kg HE explosion. Note: In nuclear explosions approximately half the energy goes directly into radiation hence 1 kt NE ~ 0.5 kt HE equivalent acoustic yield.

surface source. This source altitude effect means that treating the p_0/p term as a constant in Equation (2) is incorrect, instead the magnitude of this term may vary between events as the various bolides detonate at varying altitudes.

As the bolide curve represents an average of all the observed bolide infrasound events, we may apply the p_0/p correction for various source altitudes and produce an estimate for the average altitude for bolide infrasound energy deposition. Applying the p_0/p term to the bolide curve using pressure values from the 1978 U.S. Standard Atmosphere (U.S. Committee on Extension to the Standard Atmosphere, 1976) for altitudes of 10–40 km, it is observed that the ''corrected curves'' cross the nuclear/high explosive curves between the altitudes of 20 and 30 km (Figure 5). This altitude interval corresponds well with observed terminal altitudes for 0.1–1 m diameter bolides (e.g. Docobo and Ceplecha, 1999; Borovička and Kalenda, 2003).

The differing slope between the bolide curve and explosion values is possibly a consequence of the deeper penetration for more energetic bolides. These bigger events will generally occur at smaller scaled ranges; indeed nearly all events with scaled range less than 126 km have total yields determined from satellite data of > 0.5 kt. Penetrating deeper into the atmosphere they will have less attenuated amplitude signals and this be closer to the ''ground'' curves. Ideally one would like to evaluate this correction directly from observations; unfortunately the terminal altitudes for most of the observations in the current dataset remain an unknown parameter. Instead an alternative approach would be to separate the large and small events and evaluate their slopes independently as a test of the deeper penetration hypothesis. However this test must wait for the number of observed bolides to accumulate as the dataset still somewhat limited in the number of very energetic events.

Acknowledgements

The authors would like to thank Catherine Woodgold and David McCormack for their assistance in obtaining the infrasound data that were necessary for this study. We also thank the United States Department if Defence for making available satellite energy estimates.

References

Ben-Menahem, A.: 1975, *Phys. Earth Plan. Sci.* **11**, 1–35.

Borovička, J. and Kalenda, P.: 2003, *Meteorit. Plan. Sci.* **38**, 1023–1043.

Brown, P. G., Whitaker R. W., and ReVelle D. O.: 2002a, *Geophys. Res. Lett.*, **29**, 1–4.

Brown, P. G., Spalding R. E., ReVelle D. O., Tagliaferri E., and Worden, S. P.: 2002b, *Nature* **420**, 314–316.

Brown, P. G., ReVelle D. O., Tagliaferri E., and Hildebrand A. R.: 2002c, *Meteorit. Plan. Sci.* **37**, 661–675.

Brown P. G., Kalenda P., ReVelle D. O., and Borovička J.: 2003, *Meteorit. Plan. Sci.* **38,** 989–1003.

Brown, P., Pack D., Edwards W. N., ReVelle, D. O., Yoo B. B., Spalding R.E., and Tagliaferri E.: 2004, *Meteorit. Plan. Sci.* **39**, 1781–1796.

Tagliaferri, E., Spalding, R., Jacobs, C., Worden, S. P., and Erlich, A.: 1994, *Hazards due to Comets and Asteroids*, The University of Arizona Press, pp. 199–220.

Ceplecha, Z., Borovička, J., Elford, W. G., ReVelle, D. O., Hawkes, R. L., Porubčan, V., and Šimek, S.: 1998, Space Science Reviews, **84**, 327–471.

Docobo, J. and Ceplecha, Z.: 1999, *Astron. Astrophys. Suppl. Ser.* **138**, 1–9.

Dziewonski, A. and Hales, A.: 1972, in Bolt B. (ed.), *Methods in Computational Physics* (vol. 11), Academic Press, New York, pp. 39–84.

Hedin, A. E., Fleming, E. L., Manson, A. H., Schmidlin, F. J., Avery S. K., Clark R. R., Franke S. J., Fraser G. J., Tsuda T., Vial F., and Vincent R. A.: 1996, *J. Atmos. Terr. Phys.* **58**, 1421–1447.

Hildebrand, A. R., Brown, P., Crawford, D., Boslough, M., Chael, E., ReVelle, D., Doser, D., Tagliaferri, E., Rathbun, D., Cooke, D., Adcock, C, and Karner, J.: 1999, *LPSC XXX*, Abstract #1525, Lunar and Planetary Science Institute, Houston.

Pichon, A. L., Guerin, J. M., Blanc, E. and Reymond, D.: 2002, *JGR* **107**, 4709, doi:10.1029/2001JD001283.

Reed, J. W.: 1977, *J. Acous. Soc. Amer.* **61**, 39–47.

ReVelle, D. O.: 1976, *JGR* **81**, 1217–1230.

ReVelle, D. O., and Whitaker, R. W.: 1997, *LA-UR-96–3594*, 1–15.

ReVelle, D. O., Whitaker, R. W., and Armstrong, W. T.: 1998, *LA-UR-98–2893*, 1–12.

Spurny, P., Oberst, J., and Heinlein, D.: 2003, *Nature* **423**, 151–153.

United States Committee on Extension to the Standard Atmosphere: 1976, *U.S. Standard Atmosphere, 1976*, U.S. Government Printing Office , Washington.

Webb, W. L.: 1966, *Structure of the Stratosphere and Mesosphere*, Academic Press, New York.